Available online at BCREC website: https://bcrec.id

Bulletin of Chemical Reaction Engineering & Catalysis, 15 (1) 2020, 66-73

Research Article

Carbon Waste Powder Prepared from Carbon Rod Waste of Zinc-Carbon Batteries for Methyl Orange Adsorption

Fitria Rahmawati[1]*, Viona Natalia[1], Agung T. Wijayanta[2], Koji Nakabayashi[3], Jin Miyawaki[3], Siti Rondiyah[1]

[1]Research Group of Solid State Chemistry and Catalysis, Chemistry Department, Sebelas Maret University, Jl. Ir. Sutami 36 A, Kentingan Surakarta, Indonesia
[2]Research Group of Sustainable Thermofluids, Mechanical Engineering, Sebelas Maret University, Jl. Ir. Sutami 36 A, Kentingan, Surakarta, Indonesia
[3]Department of Advanced Device Materials, Institute for Materials Chemistry and Engineering, Kyushu University, 6-1 Kasuga-koen, Kasuga-shi, Fukuoka 816-8580, Japan

Received: 17th June 2019; Revised: 1st September 2019; Accepted: 3rd September 2019; Available online: 28th February 2020; Published regularly: April 2020

Abstract

A research on the preparation of Carbon Waste Powder, CWP, was conducted and made from carbon rod waste which was extracted from used zinc-carbon batteries. This research was an effort to overcome environmental problem caused by battery waste by converting into adsorbent for methyl orange (MO) that frequently used by textile industries. The prepared powder was then analyzed to understand its characteristic peaks, crystallinity, and to compare the properties with other carbonaceous forms, i.e. a commercial Carbon Paper (CP), and a commercial meso- carbon micro-beads (MCMB). The analysis found that CWP is dominated by graphitic carbon. An adsorption experiment was then conducted to study their adsorption ability to methyl orange solution. The result found that those three carbonaceous materials have the ability to adsorb methyl orange with different activities. MCMB has the highest adsorption capacity of 0.197 mg.g^{-1}. Meanwhile, CWP and CP show adsorption capacity of 0.066 mg.g^{-1} and 0.062 mg.g^{-1}, respectively. Methyl orange adsorption on CWP and CP were under second order, which means the adsorption could be four times faster as the MO solution doubled. Moreover, the rate constant of MO adsorption on CWP is 8×10^{-4} min^{-1}, which was higher than the rate constant of MO adsorption on CP. It confirmed that the CWP can be used as a promising adsorbent for dye waste water.

Keywords: Adsorption; Carbon rod waste; Carbon waste powder; Methyl orange

How to Cite: Rahmawati, F., Natalia, V., Wijayanta, A.T., Nakabayashi, K., Miyawaki, J., Rondiyah, S. (2020). Carbon Waste Powder Prepared from Carbon Rod Waste of Zinc-Carbon Batteries for Methyl Orange Adsorption. *Bulletin of Chemical Reaction Engineering & Catalysis*, 15(1): 66-73 (doi:10.9767/bcrec.15.1.5148.66-73)

Permalink/DOI: https://doi.org/10.9767/bcrec.15.1.5148.66-73

1. Introduction

Dye waste water has become an environmental problem due to the production of paper, textiles, gasoline, cosmetics, food industries, etc. [1]. Dye wastes are toxic, hazardous, and non-biodegradable [2], that may cause the destruction of aquatic living organisms [3]. As one of the dye compound, methyl orange (MO) is known as an azo anionic type that contains of −N=N− chromophore group and aromatic structure [4,5]. The chromo-

* Corresponding Author.
E-mail: fitria@mipa.uns.ac.id (F. Rahmawati);
Telp: +62-271-663375, Fax: +62-271-663375

phore and aromatic group are difficult to undergo auto-degradation. Specific treatment is required to overcome the waste water, such as through membrane filtration method [6], chemical oxidation [7], adsorption [1], and also coagulation. Adsorption might be a good choice due to the ease of preparation and simplicity of the reactor design [8,9]. It is known that activated carbon is the most popular adsorbent for various dye waste water [10]. The performance of MO adsorption follows a pseudo second order [11]. Another carbon- based adsorbent is carbon nanotubes that also has the ability to adsorb MO molecules from its aqueous solution [3].

In another side, year by year solid waste batteries increases due to high demand on portable electronic devices. Primary battery still dominates the market, in which 80 % battery selling in Europe, mostly alkaline and zinc-carbon battery [12]. Around 160,000 tons of batteries enter the European Union every year [13]. Environmental Protection Agency (EPA) reveals that each year Americans purchase three billion dry cell battery to power radios, toys, cellular phones, watches, and portable power tools [14].

In order to reduce the waste impact to environment, some efforts must be done by reusing some components in battery waste, such as to reuse the carbon rod of zinc-carbon battery for photo catalyst substrate in hydrogen production [15], and also for raw material in graphene oxide synthesis [16]. This research also has used the carbon rods of zinc-carbon battery waste for preparing adsorbent powder, named as carbon waste powder, CWP. The novelty of this work is its raw material, which is unique for creating a specific adsorbent powder. The powder was then applied to adsorb methyl orange, MO, from its aqueous solution. The adsorption performance was compared to other carbonaceous forms, i.e. carbon paper, CP, and meso-carbon micro-beads, MCMB. Adsorption equilibrium study was conducted to determine the adsorption capacity ($mg.g^{-1}$). Kinetics of adsorption determines the adsorption rate, the rate constant, and the order of adsorption. Meanwhile, isotherm explains the adsorption type between single or multi-layer and also predicts the type of interaction between adsorbate molecules and the prepared carbon as the adsorbent. The present effort contributes to the understanding of characteristics of the proposed adsorbent derived from waste material aims to provide an environmental protection.

2. Materials and Methods

2.1 Material Preparation and Characterization

Carbon waste powder, CWP, was produced from carbon rod waste extracted from a zinc-carbon battery (ABC battery, Indonesia). The carbon rods waste were cleaned by dipping in ethanol liquid and then washed with distilled water followed by drying at 105 °C for 1 h [15], and then crushed into powder. The prepared powder was then analyzed by XRD (Rigaku Mini Flex 600 X-Ray diffraction instrument with Cu-Kα radiation (λ = 1.5406 Å) in 2θ range of 10-70°. A commercial MCMB powder (MTI scientific, bead size around 6-52 μm) and a commercial carbon paper (*the Fuel Cell store*, cut into pieces with a size of 1×1 cm^2) were used for comparison. The MCMB and CP were also analyzed by XRD to identify the carbonaceous peaks. Scanning Electron Microscopy, SEM (FEI Inspect s50) analyzed surface morphology as well as to estimate the particle size by applying Measure IT software (a free edition). Adsorption isotherm, total pore volume ($cm^3.g^{-1}$), and surface area ($m^2.g^{-1}$) of the prepared CWP were identified by applying a BET instrument (NOVA touch 4LX).

2.2 Adsorption Experiment

The aqueous MO stock solution was prepared by dissolving 100 mg MO into 1000 mL of deionized water (Merck, Germany with molecular weight 327.34 $gmol^{-1}$). The adsorption experiment was conducted at room temperature at the various contact time, and the MO solution concentration. In order to get the maximum absorbance of MO, a various concentration of MO solution was prepared at 0, 2, 4, 6, 8, and 10 ppm, and the solution then being scanned between 100-700 nm of light wavelength in a UV-Vis spectrophotometer (Perkin Elmer Lambda 25). It is found that MO reveals a maximum absorbance at 465 nm.

Adsorption experiment was conducted by poured a 0.5 g adsorbent into 50 mL of 100 ppm MO solution in a flacon. The mixture was then shaken for 0-300 minutes, in which, to collect data, 2 mL of solution was diluted to 25 mL, which was then analyzed by UV-Vis spectrophotometer at 465 nm. The optimum time of adsorption was determined by plotting absorbance, A, data to the time of adsorption, t (min), and the optimum time was reached when the absorbance value starts to be constant. The optimum time was then used for the MO adsorption isotherm calculation. The MO adsorption

isotherm was studied at 2, 4, 6, 8, and 10 ppm of MO solution adsorbed onto 0.5 g adsorbent. The initial rate, or the rate of adsorption before reaching equilibrium was used for kinetics study of each adsorption process. Data of MO adsorbed onto the absorbents, C_{ads} (mg.L^{-1}), was used to understand the pattern of adsorption on each adsorbent, and confirms the suitability with kinetics study.

The adsorbed amount of MO at equilibrium, q_e (mg/g) was calculated by Equation (1) [17]:

$$q_e = \frac{(C_o - C_e)V}{W} \quad (1)$$

C_o and C_e (mg.L^{-1}) are initial and the equilibrium concentration of MO solution, respectively; W (g) is the weight of adsorbent used and V (L) is the volume of solution. Langmuir and Freundlich's isotherm was applied to analyze the adsorption data. The material analysis was conducted by applying FTIR spectrophotometer (Shimadzu Infrared Prestige 21 with KBr pellet as substrate) to understand the change in their functional group at before and after adsorption.

Enthalpy of adsorption, ΔH_{ads} was determined by plotting ln C_e to 1/T (K^{-1}) following Clausius-Clapeyron equation (eq. 2) [18], in which T is temperature (K), R is gas constant 8.314 J.mol^{-1}.K^{-1} and C is a constant, available as intercept in the linear regression. Data for thermodynamics plot was found by conducting adsorption experiment at the time of equilibrium under room temperature (28 °C), 30, 40, and 50 °C. The adsorption was conducted twice for each temperature. The result was presented as average value with standard deviation of each.

$$\ln C_e = -\frac{\Delta H}{RT} + C \quad (2)$$

3. Results and Discussion

X-ray diffraction pattern of the prepared carbon waste powder is depicted in Figure 1(a), compared to the diffraction pattern of the MCMB and CP. A broad peak lying at 2θ of 22-25° appears in the CWP diffraction pattern indicates the presence of amorphous carbon as it was also found in the previous research [15]. CP diffraction pattern shows very low intensity peak at around 2θ of 24.5° indicates the presence of amorphous carbon. The amorphous phase of CP is confirmed by the broad and noisy diffraction pattern compare to the other carbonaceous phases. Meanwhile, CWP and

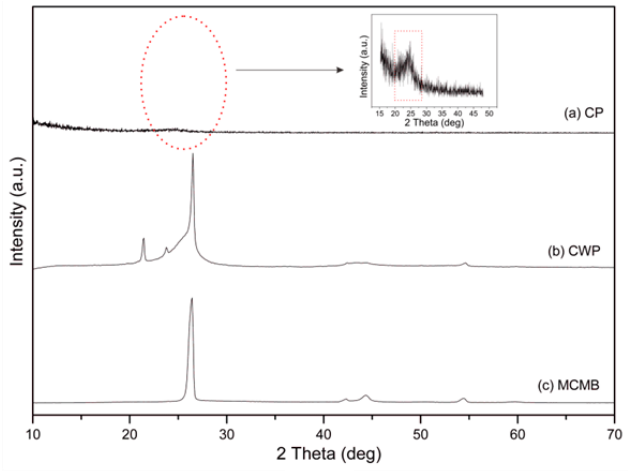

(a)

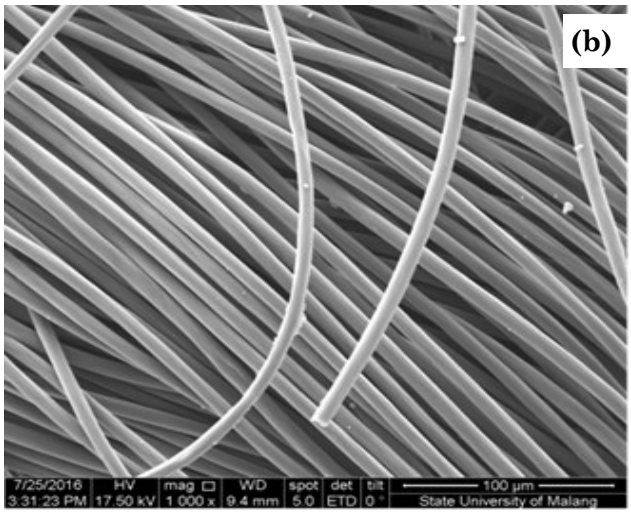

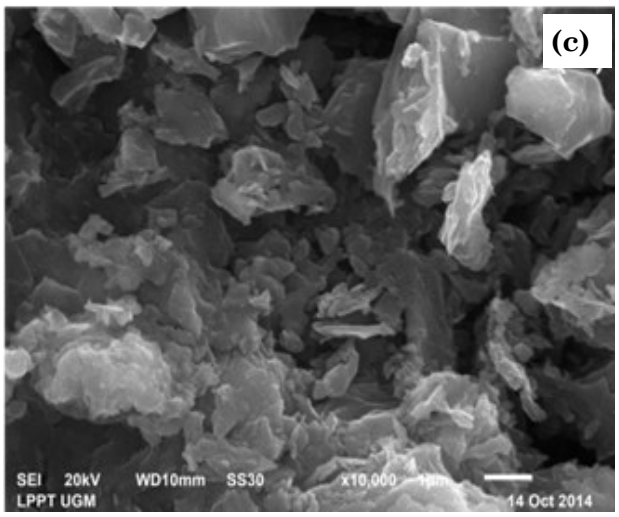

Figure 1. (a) The diffraction pattern of the carbon from carbon rod waste (CWP) in comparison with carbon paper (CP) and commercial graphite (MCMB) and (a) SEM images of carbon paper and (c) carbon waste powder.

MCMB show a strong peak at 2θ of 26.3° which is identified as graphitic carbon, as well as peaks at 2θ of 44.23° and 54.61°. The graphitic carbon peaks are in agreement with standard graphite diffraction of ICSD#53781.

Morphological analysis by SEM resulted in images as depicted in Figure 1(b) and (c). Carbon paper as illustrated in Figure 1(b) describes a homogenous wire with a diameter of around 5.5 μm. Meanwhile, carbon waste powder shows a rough and non-homogenous surface morphology as describes in Figure 1(c).

The adsorption of MO molecules by CWP is shown by the changes in the FT-IR spectra (Figure 2) at before and after adsorption. The CWP spectrum after adsorption exhibits characteristic peaks at 1552.76 cm^{-1} and 1083.08 cm^{-1}, that indicate N=N vibration from the azo bond, and S=O vibration, respectively [19]. Meanwhile, the peaks at 1053.18 cm^{-1}, 775.00 cm^{-1}, and 622.07 cm^{-1} are attributed to C−H stretching of aromatic rings. The peak at 555.52 cm^{-1} corresponds to C−S stretching vibration [19]. All peaks are relatively weak due to low MO solution concentration, i.e. 10 $mg.L^{-1}$, allowing a limit quantity of MO molecules to be adsorbed. A peak at around 3400 cm^{-1} that provide in all spectrum refers to O−H stretching of water molecules. Another peak at 2800-3000 cm^{-1} corresponds to the antisymmetric and symmetric stretching vibration of $-CH_3$ [20].

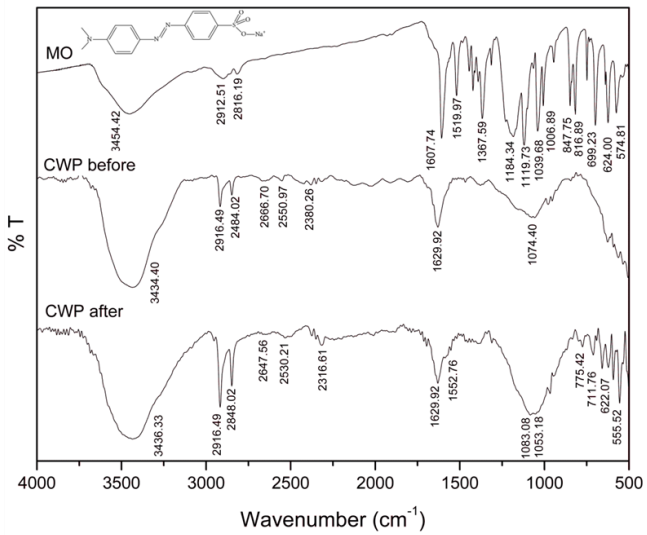

Figure 2. The characteristic pattern of FTIR spectra of the MO, CWP before adsorption and after adsorption of MO after 300 minutes with concentration MO of 10 $mg.L^{-1}$.

Adsorption test produced a plot of absorbance, *A* to time, *t* (min) as depicted in Figure 3 (a). The absorbance plot confirms that the adsorption reached equilibrium after 200 min MO adsorption to CWP. The adsorption rate was fast at the first 50 min before it turned into a slow rate and then reached equilibrium. In order to compare adsorption performance between CWP, CP, and MCMB, a plot of the adsorbed amount ($mg.g^{-1}$ adsorbent) versus time (min) is described in Figure 3 (b). The plot shows that MCMB provides the highest adsorption capacity value, i.e. 0.197 $mg.g^{-1}$. Meanwhile, the adsorption capacity of MO to CWP and CP are 0.066 and 0.062 $mg.g^{-1}$, respectively.

Kinetics study was taken at before the adsorption reach equilibrium, or at initial rate adsorption. By applying first and second order rate law, it was found that adsorption of MO to CWP and CP follow second order rate law with a rate constant of 8×10^{-4} min^{-1} and 2×10^{-4} min^{-1}, respectively. Meanwhile, MO adsorption to MCMB follows first order with a rate constant of 7×10^{-4} min^{-1}. It means that, when the MO concentration increases twice, the adsorption

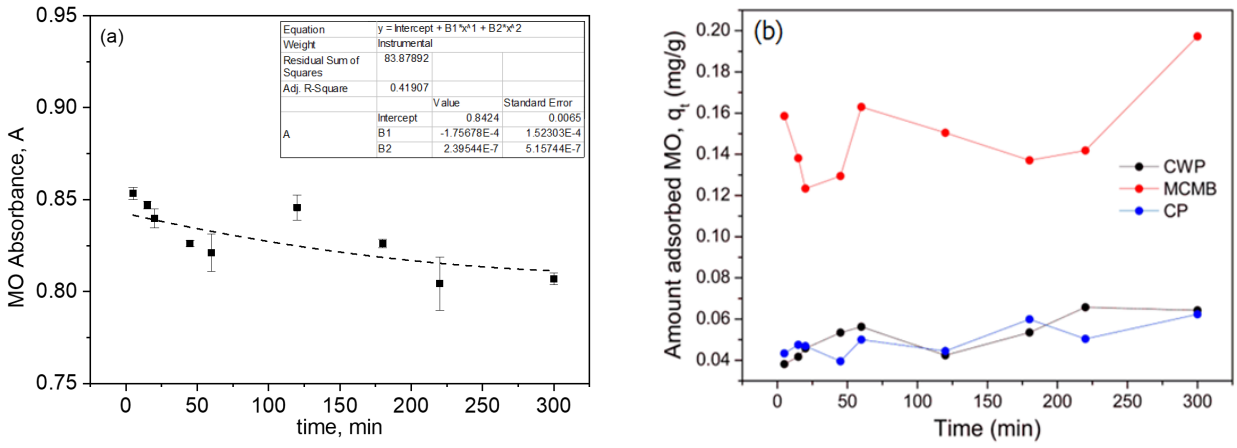

Figure 3. (a) Plot of absorbance to the time of adsorption on CWP, and (b) Plot of adsorption amount to the time of adsorption with the various adsorbent. The MO solution is 10 $mg.L^{-1}$.

on CWP and CP will be four times faster. However, the adsorption rate will increase only twice when MCMB is used as an adsorbent. It is proved by conducting adsorption at a various initial concentration of MO solution. The result can be checked in Figure 4, in which Kinetics parameters are listed in Table 1. Figure 4 shows that when the MO concentration was 2 ppm, MO adsorption onto CWP was less than the adsorption onto MCMB. However, by MO concentration increasing, the adsorption onto CWP shows a higher increment than MO onto MCBM. Meanwhile, MO adsorption onto CP has similar type with MO adsorption onto MCMB, even though kinetics study found that the MO adsorption onto CP follows second order kinetics. It indicates that high MO desorption from CP surface due to low interaction between the molecules with the surface, as it is confirms that the adsorption follows Freundlich isotherm (Table 2). Freundlich isotherm fits with a multilayer adsorption supported by physical adsorption.

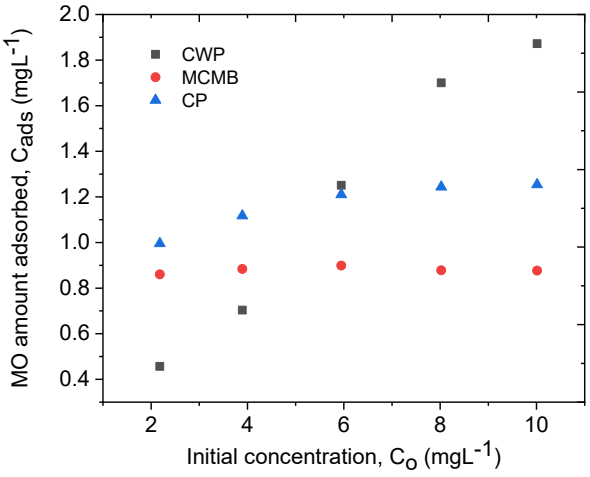

Figure 4. Plot of MO amount adsorbed, C_{ads}, at a various initial MO concentration, C_o

Adsorption capacity at every contact time refers to q_e (mg.g^{-1}) was plotted to Langmuir and Freundlich Isotherm (Equation (3) and (4) [17,21]. The isotherm study how is the distribution of molecular adsorption on adsorbent when the adsorption reach equilibrium [11].

$$\frac{C_e}{q_e} = \frac{1}{q_m K_L} + \frac{C_e}{q_m} \quad (3)$$

q_m is maximum monolayer capacity of adsorbent (mg.g^{-1}), C_e is the equilibrium concentration of MO solution (mg.L^{-1}) and K_L is Langmuir adsorption constant (L.mg^{-1}). The Langmuir adsorption isotherms describe quantitatively the formation of a monolayer adsorbate on the outer surface of the adsorbent

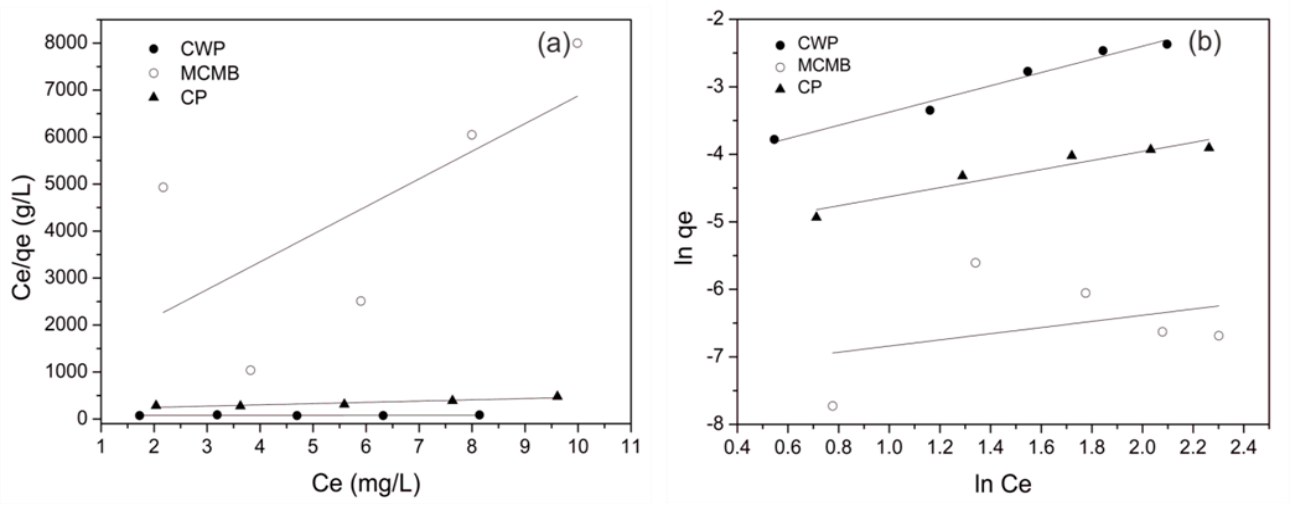

Figure 5. The linear of plot (a) Langmuir and (b) Freundlich isotherms.

Table 1. The kinetics parameters of rate constant (k) and the linearity coefficient (R^2) for CP, CWP, and MCMB adsorbent.

No.	Materials	1st order kinetics		2nd order kinetics	
		k_1	R^2	k_2	R^2
1	CP	1×10^{-4}	0.5765	2×10^{-4}	0.9877
2	MCMB	7×10^{-4}	0.9989	11×10^{-4}	0.9984
3	CWP	2×10^{-4}	0.6394	8×10^{-4}	0.9020

[22]. The values of q_m and K_L were calculated from the slope and intercept of the Langmuir plot of C_e/q_e versus C_e as shown by Figure 5.

Freundlich adsorption isotherms (equation (4)) describes the heterogeneity of the adsorbent and multi-layer coverage of adsorbate [22].

$$\ln q_e = \ln K_F + \frac{1}{n} \ln C_e \qquad (3)$$

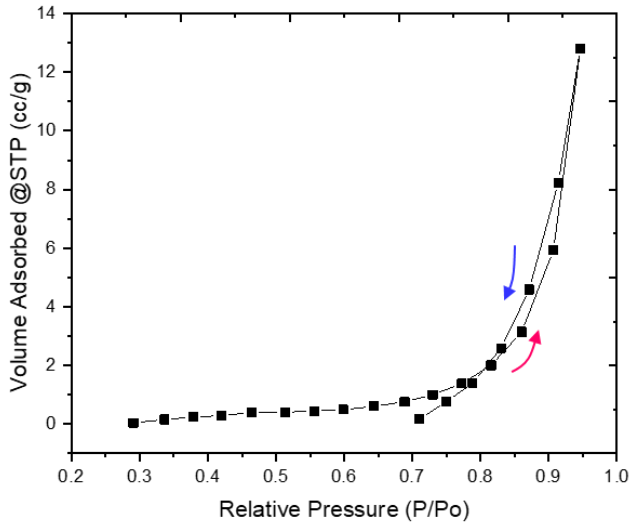

Figure 6. Adsorption isotherm profile of N_2 gas adsorption to Carbon Waste Powder, CWP at 41.58 °C ambient temperature. Red arrow refers adsorption, and blue arrow refers desorption.

K_F and n are the Freundlich isotherms constant. The higher value of K_F and n are indicated higher adsorption capacity and stronger adsorption bond between adsorbate and adsorbent, respectively [17]. The values of K_F and n is calculated from the intercept and slope of the plot ln C_e versus ln q_e. The linear plot of Langmuir and Freundlich are shown in Figure 5, meanwhile the isotherm parameters are listed in Table 2. The correlation coefficient (R^2) clarify the suitability of isotherm application.

The K_F and n values of MO sorption on CWP are 0.0129 (mg/g) $(L/mg)^{1/n}$ and 0.9770, respectively. The value of $1/n$ = 0.9770 as listed in Table 2 indicating the appropriate adsorption of MO. In which, the value below 1 means normal adsorption, while the $1/n$ value above 1 indicates cooperative adsorption [22,23].

Table 2 confirms that MO adsorption on CWP and CP comply with Freundlich isotherm, with a coefficient of 0.9762 and 0.9239, respectively. Meanwhile, MO adsorption on MCMB follows Langmuir isotherm. The result indicates that MO molecules are adsorbed to MCMB as a single layer and MO molecules are adsorbed to CWP and CP as a multilayer. The results are in line with the kinetics study, in which MO adsorption on MCMB follows the 1st order. Even though MO concentration contributes to the adsorption capacity, the contribution will not as high as adsorption on

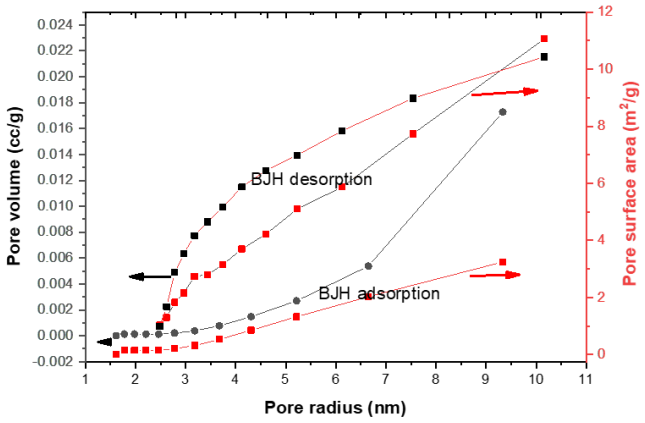

Figure 7. The adsorption and desorption BJH pore size distribution of N_2 gas on CWP powder.

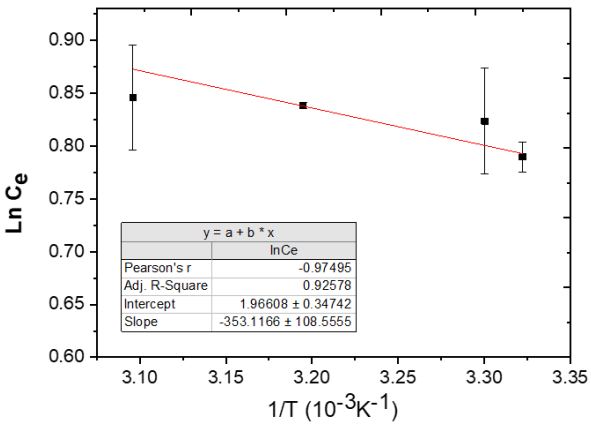

Figure 8. Clausius - Clapeyron plot for the determination of adsorption enthalpy.

Table 2. Parameters of the Langmuir and Freundlich isotherms for various adsorbent

Sample	Langmuir			Freundlich		
	q_m (mg.g^{-1})	K_L(L.mg^{-1})	R^2	K_F (mg.g^{-1}) (L.mg^{-1})$^{1/n}$	$1/n$	R^2
CWP	2.2261	0.0284	0.0216	0.0129	0.9770	0.9762
MCMB	0.0017	0.5959	0.4427	0.0006	0.4562	0.1212
CP	0.0374	0.1376	0.8882	0.0050	0.6698	0.9239

CWP and CP, which have four times higher contribution. Monolayer adsorption may have a stronger interaction between adsorbate-adsorbent. However, the molecules adsorb are less quantity than multilayer adsorption.

The multilayer adsorption on CWP was further analyzed by conducting a BET isotherm analysis under N_2 gas flows. The isotherm profile is described in Figure 6. It shows that the adsorption capacity reached 12.8 cc.g^{-1} when nitrogen supplied up to 0.95 of relative pressure. Completed-N_2 desorption occurred when the relative partial pressure dropped close to 0.7 relative pressure. A small hysteresis loop between adsorption-desorption curve indicates a multilayer MO adsorption on the CWP surface, in which adsorbate-adsorbent interaction usually low in a multilayer term. It causes desorption to occur faster than adsorption. It may also be caused by irreversible adsorption, in which adsorption itself distord the structure of adsorbent [24]. Structure distortion of adsorbent may change pore size of adsorbent, change the surface area, as well as change adsorption capacity from monolayer to multilayer. Structure distortion may also cause the different BJH pore size distribution based on adsorption and desorption result. Both curves of results is described in Figure 7. BJH calculation resulted in the total pore volume of 1.9853×10^{-2} cm^3.g^{-1} at relative pressure of 0.9465, and the average pore radius is 7.229 nm.

Thermodynamics study by plotting adsorption data to Clausius-Clapeyron equation (Figure 8), found that the adsorption occurred endothermically, with enthalpy change value, ΔH of 2.936 ± 0.903 kJ.mol^{-1}. The energy of adsorption is within low energy category, or the adsorption of MO on CWP powder can be claimed as physisorption. The adsorption energy less than 8 kJ.mol^{-1} is physisorption type, in between 8-16 kJ mol^{-1} is ion-exchange, and over 16 kJ.mol^{-1} is categorized as chemisorption [25].

4. Conclusions

Carbon Waste Powder, CWP, prepared from carbon rods extracted from zinc-carbon battery waste has the ability to adsorb methyl orange, MO, in aqueous solution. Kinetics study reveals that the MO adsorption to CWP follows second order with a rate constant of 8×10^{-4} min^{-1}. The rate constant is greater than the adsorption on carbon paper, CP, or meso-carbon micro-bead, MCMB. Even though, the adsorption capacity is 0.066 mg.g^{-1} which is lower than the adsorption capacity of MCMB to MO solution, i.e. 0.197 mg.g^{-1}. MO adsorption on CWP fits well with Freundlich isotherm, confirming multilayer coverage of MO molecules on CWP surface. The adsorption occurred through physisorption. Initial MO concentration significantly affect the adsorption rate and amount of adsorption.

Acknowledgment

This research was a part of research PNBP Sebelas Maret University, Indonesia, contract number 259/UN27/HK/2018. This research was also supported partially by a Bilateral Exchange Program JSPS/DG-RSTHE Joint Research Project 2018 grant, from the Japan Society for the Promotion of Science. Authors acknowledged these financial supports.

References

[1] Gupta, V.K., Kumar, R., Nayak, A., Saleh, T.A., Barakat, M.A. (2013). Adsorptive removal of dyes from aqueous solution onto carbon nanotubes: A review. *Advance Colloid and Interface Science*, 193-194, 24–34. doi:10.1016/j.cis.2013.03.003.

[2] Sharma, P., Kaur, H., Sharma, M., Sahore, V. (2011). A review on applicability of naturally available adsorbents for the removal of hazardous dyes from aqueous waste. *Environmental Monitoring Assessment*, 183, 151–95. doi:10.1007/s10661-011-1914-0.

[3] Zhao, D., Zhang, W., Chen, C., Wang, X. (2013). Adsorption of Methyl Orange Dye Onto Multiwalled Carbon Nanotubes. *Procedia Environmental Science*, 18, 890–895. doi:10.1016/j.proenv.2013.04.120.

[4] Hassanzadeh-Tabrizi, S.A., Motlagh, M.M., Salahshour, S. (2016). Synthesis of ZnO/CuO nanocomposite immobilized on γ-Al_2O_3 and application for removal of methyl orange. *Applied Surface Science*, 384, 237–243. doi:10.1016/j.apsusc.2016.04.165.

[5] Hosseini, S., Khan, M.A., Malekbala, M.R., Cheah, W., Choong, T.S.Y. (2011). Carbon coated monolith, a mesoporous material for the removal of methyl orange from aqueous phase: Adsorption and desorption studies. *Chemical Engineering Journal*, 171, 1124–1131. doi:10.1016/j.cej.2011.05.010.

[6] Liu, J., Xiong, J., Tian, C., Gao, B., Wang, L., Jia, X. (2018). The degradation of methyl orange and membrane fouling behavior in anaerobic baffled membrane bioreactor. *Chemical Engineering Journal*, 338, 719–725. doi:10.1016/j.cej.2018.01.052.

[7] Mazumder, N.A., Rano, R. (2018). Synthesis and Characterization of Fly Ash Modified

Copper Oxide (FA/CuO) for Photocatalytic Degradation of Methyl Orange Dye. *Material Today Proceeding*, 5, 2281–2286. doi:10.1016/j.matpr.2017.09.230.

[8] Gautam, R.K., Mudhoo, A., Lofrano, G., Chattopadhyaya, M.C. (2014). Biomass-derived biosorbents for metal ions sequestration: Adsorbent modification and activation methods and adsorbent regeneration. *Journal of Environmental Chemical Engineering*, 2, 239–259. doi:10.1016/j.jece.2013.12.019.

[9] De Gisi, S., Lofrano, G., Grassi, M., Notarnicola, M. (2016). Characteristics and adsorption capacities of low-cost sorbents for wastewater treatment: A review. *Sustainable Materials & Technology*, 9, 10–40. doi:10.1016/j.susmat.2016.06.002.

[10] Ramakrishna, K.R., Viraraghavan, T. (1997). Dye removal using low cost adsorbents. *Water Science Technology*, 36, 189–196. doi:10.1016/S0273-1223(97)00387-9.

[11] Gong, R., Ye, J., Dai, W., Yan, X., Hu, J., Hu, X. (2013). Adsorptive removal of methyl orange and methylene blue from aqueous solution with finger-citron-residue-based activated carbon. *Industrial & Engineering Chemistry Research*, 52, 14297–14303. doi:10.1021/ie402138w.

[12] Lang, J., Matejka, V. (2013). Graphite / titanium dioxide composite. *Nanocon*, Brno, Czech Republic, EU: 2013. doi:10.1039/c3bm60192g.

[13] Anonym. (2018). Batteries & Accumulators. http://ec.europa.eu/environment/waste/batteries/index.htm (accessed April 8, 2018).

[14] Laughlin, R.B. (2008). Environmental Protection Agency - Battery Waste. http://large.stanford.edu/publications/coal/references/epa/.

[15] Rahmawati, F., Yuliati, L., Alaih, I.S., Putri, F.R. (2017). Carbon rod of zinc-carbon primary battery waste as a substrate for CdS and TiO2 photocatalyst layer for visible light driven photocatalytic hydrogen production. *Journal of Environmental Chemical Engineering*, 5, 2251-2258. doi:10.1016/j.jece.2017.04.032.

[16] Rahmawati, F., Prasasti, B.L.W., Mudjijono, M. (2018). Graphene Oxide from Carbon Rod Waste. *IOP Conference Series: Material Science and Engineering*, 333, 012012. doi:10.1088/1757-899X/333/1/012012.

[17] Rattanapan, S., Srikram, J., Kongsune, P. (2017). Adsorption of Methyl Orange on Coffee grounds Activated Carbon. *Energy Procedia*, 138, 949–954. doi:10.1016/j.egypro.2017.10.064.

[18] Wang, T., Shen, C., Wang, N., Dai, J., Liu, Z., Fei, Z. (2019). Adsorption of 3-Aminoacetanilide from aqueous solution by chemically modified hyper-crosslinked resins: Adsorption equilibrium, thermodynamics and selectivity. *Colloids and Surfaces A Physicochemical and Engineering Aspect*, 575, 346–351. doi:10.1016/j.colsurfa.2019.05.029.

[19] Umamaheswari, C., Lakshmanan, A., Nagarajan, N.S. (2018). Green synthesis, characterization and catalytic degradation studies of gold nanoparticles against congo red and methyl orange. *Journal of Photochemistry and Photobiology B Biology*, 178, 33–39. doi:10.1016/j.jphotobiol.2017.10.017.

[20] Li, P., Song, Y., Wang, S., Tao, Z., Yu, S., Liu, Y. (2015). Enhanced decolorization of methyl orange using zero-valent copper nanoparticles under assistance of hydrodynamic cavitation. *Ultrasonic Sonochemistry*, 22, 132–138. doi:10.1016/j.ultsonch.2014.05.025.

[21] Zhai, L., Bai, Z., Zhu, Y., Wang, B., Luo, W. (2018). Fabrication of chitosan microspheres for efficient adsorption of methyl orange. *Chinese Journal of Chemical Engineering*, 26, 657–666. doi:10.1016/j.cjche.2017.08.015.

[22] Dada, A.O. (2012). Langmuir, Freundlich, Temkin and Dubinin–Radushkevich Isotherms Studies of Equilibrium Sorption of Zn^{2+} Unto Phosphoric Acid Modified Rice Husk. *IOSR Journal of Applied Chemistry*, 3, 38–45. doi:10.9790/5736-0313845.

[23] Mohan, S.V,, Karthikeyan, J. (1997). Removal of lignin and tannin colour from aqueous solution by adsorption onto activated charcoal. *Environmental Pollution*, 97, 183–187. doi:10.1016/S0269-7491(97)00025-0.

[24] Lapham, D.P., Lapham, J.L. (2019). Gas adsorption on commercial magnesium stearate: The origin of atypical isotherms and BET transform data. *Powder Technology*, 342, 676–689. doi:10.1016/j.powtec.2018.10.035.

[25] Shen, S., Guishen, L., Pan, T., He, J.Z., Guo, Z. (2011). Selective adsorption of Pt ions from chloride solutions obtained by leaching chlorinated spent automotive catalysts on ion exchange resin Diaion WA21J. *Journal of Colloid and Interface Science*, 364, 482–489. doi:10.1016/j.jcis.2011.08.043.